

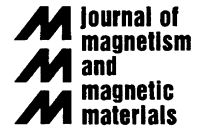


ELSEVIER

Available online at www.sciencedirect.com

SCIENCE @ DIRECT®

Journal of Magnetism and Magnetic Materials 266 (2003) 194–199



www.elsevier.com/locate/jmmm

Temperature dependent integral generalized Delta-M plots and interactions in cobalt nanoparticle systems

L. Spinu^{a,*}, A. Stancu^b, L.D. Tung^c, J. Fang^c, P. Postolache^b, C.J. O'Connor^c

^a *Physics Department, Advanced Materials Research Institute, University of New Orleans, 2000 Lakeshore Drive, New Orleans, LA 70148, USA*

^b *Faculty of Physics, "Al. I. Cuza" University, Iasi 6600, Romania*

^c *Advanced Materials Research Institute, University of New Orleans, New Orleans, LA 70148, USA*

Received 20 September 2002; received in revised form 22 April 2003

Abstract

The effect of inter-particle interaction in samples of Co nanoparticles dispersed in different volume fractions in a wax matrix was studied. The evolution of interaction intensity in the Co nanoparticle systems as a function of temperature was determined by measuring the integral generalized Delta-M curves. These experimental curves do not require AC demagnetized states of the sample, which is an important simplification of the experimental procedure. The results are analyzed with a generalized moving Preisach model.

© 2003 Elsevier B.V. All rights reserved.

PACS: 75.60.-d; 75.60.Ej; 75.75.+a

Keywords: Delta-M plot; Generalized Delta-M plot; Nanoparticle system

1. Introduction

The dynamics of magnetic nanoparticle systems is a subject of considerable interest due to their fundamental and technological interest [1]. The properties of such systems are strongly modified compared to the bulk, due to granular texture and the small size of the grains. On one hand, thermal relaxation of the magnetic moment of the particles, i.e. superparamagnetic relaxation, can occur. On the other hand, magnetic inter-particle

interactions always exist in fine particle systems, and the demand for high-density recording media requires high packing densities that make the role of inter-particle interactions even more important in these magnetic systems. The combined effect of thermal relaxation and interparticle interactions is the most important feature that must be addressed in studying the properties of magnetic nanoparticle assemblies. Consequently, much theoretical and experimental work has been devoted to understand and to assess the role of interactions on the magnetic properties of fine particle systems. In this paper, we present an experimental and theoretical study of evaluating interparticle interactions in nanoparticle systems based on integral

*Corresponding author. Tel.: +1-504-280-3218; fax: +1-504-280-3185.

E-mail address: lspinu@uno.edu (L. Spinu).

generalized Delta-M (IGDM) plots [2,3]. The advantage of using the IGDM for evaluating the interactions comes from the fact that this procedure it is not affected by the uncertainty of the initial state of the magnetic system as it is the case for the standard Delta-M plot [4]. It is well known that the regular Delta-M plots require measuring the isothermal remanent magnetization (IRM) curve starting from an AC demagnetized state [5]. It was shown that depending on the initial state, AC demagnetized or thermal demagnetized, the resulting Delta-M plots for the same magnetic system can be either negative or positive, respectively [4], and this can conduct to misleading interpretations. For magnetic nanoparticle systems the remanent curves can be measured only in the blocked state that usually is found at low temperatures. Technically it is very difficult to obtain an accurate initial AC demagnetized state at low temperatures and that it is why using a procedure such as IGDM for evaluating the interactions is important.

2. Experimental setup. Samples. Experimental results

In order to investigate the role of the interactions, we performed experiments at various temperatures on samples of Co nanoparticles, dispersed in different concentrations in a wax matrix. The degree of dilution in the wax controls the average particle distance and therefore the strength of interactions. The synthesis of cobalt nanoparticles was carried out using standard organometallic reaction procedures with airless/moisture-less devices and commercially available reagents. The common approach for the synthesis of cobalt nanocrystallites is to reduce organo-cobalt salt in a non-polar solvent at relatively high temperature, capped/stabilized by some organic compounds. The experimental procedure is similar to that reported by Sun and Murray [6]. Nanoparticles were precipitated by adding ethanol to the dispersion and centrifugation under Ar atmosphere. The precipitate was then dispersed into hexane. By adding a pair of solvents consisting of hexane and ethanol and centrifugation to

fractionate the colloids from time to time, size selection was performed.

The dispersion of Co nanoparticles in the wax matrix was carried out by ultrasonically mixing the concentrated cobalt nanocrystallites in hexane with wax-hexane solution (2 min) within glovebox, followed by increasing temperature of the system to remove the solvent. The ratio of cobalt was determined based on the real amount of cobalt used and amount of wax. The results of these synthesis and separation procedures are presented in Fig. 1. The particle size and size distribution of each filtrated sample in as-prepared cobalt colloidal solution was monitored using light scattering technique (DynaPro 99 Molecular Sizing Instrument). Fig. 1 shows the Co nanoparticle size distribution, as it was obtained by light scattering. The light scattering data indicates a radius distribution of the Co nanoparticles centered on 5 nm with a tail extending to larger radii. We must mention that the “hydrodynamic size” determined by this technique is usually greater than the true physical size of the nanoparticles due of the shape and capping ligands presents on the particle’s surface. The average diameter of as prepared Co nanoparticles is 6 nm as determined by transmission electron microscopy (inset Fig. 1). In order to study the effect of interparticle interactions two

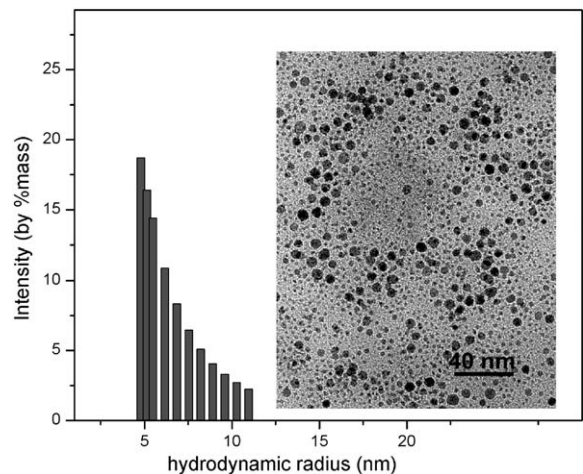


Fig. 1. The Co particle size distribution after the size selection obtained by light scattering. The inset shows the TEM image of the as-prepared Co nanoparticles.

samples were considered for this study: a sample of $C_V = 0.011$ volume fraction of Co nanoparticles dispersed in wax (Co10) and a sample containing only Co nanoparticles (Co100). The nanoparticles in both samples were from the same batch of Co nanoparticles, to make sure the same size distribution in both samples.

The effect of inter-particle interaction in the two samples was analyzed by measuring the remanent curves, DC demagnetization (DCD) and forward IRM curves. First of all, in order to evaluate the evolution of interaction intensity in the systems as a function of temperature, we have measured the IGDM at 5, 10, 15, 20, 25 and 30 K [2,3]. To produce the IGDM curves, one has to measure the classical DC demagnetized (DCD) curve and a number of IRM-type curves, referred as forward IRM curves, starting from remanent states on the DCD curve. The forward IRM curves are used to obtain the DCD' curves, as described in Ref. [2]. Essentially, we have used this methodology to avoid the necessity to produce experimentally an accurate AC demagnetized state. The forward IRM curves were measured for seven initial remanent states. The data for Co100 at 5 K are presented in Fig. 2. In order to compare the IGDMs at different temperatures they were

translated and normalized on the abscissa at the saturation remanent moment for each temperature. The translated IGDM curve was given by the formula:

$$m_{\text{IGDM}} = \int_0^{H_m} [m_{\text{DCD}'}(H) - m_{\text{DCD}}(H)] dH, \quad (1)$$

where H_m is the maximum field applied to the sample in the experiments, m_{DCD} and $m_{\text{DCD}'}$ are the magnetic moments in the DCD and DCD' processes, respectively. IGDM is represented as a function of the initial remanent state used in the IRM forward curve. In Fig. 3 the IGDM curves for the Co100 and Co10 samples are presented as a function of temperature. The Co100 sample IGDMs have a central maximum which is characteristic of a system with important static interactions [7]. The static interactions intensity is decreasing with the increase of temperature, as expected. This is determined by the fact that as the temperature is increasing more particles in the system will be in thermal equilibrium (superparamagnetic) and thus they will not contribute anymore to the static statistic (distributed) interactions (dipolar interactions between blocked magnetic moments of the particles) in the

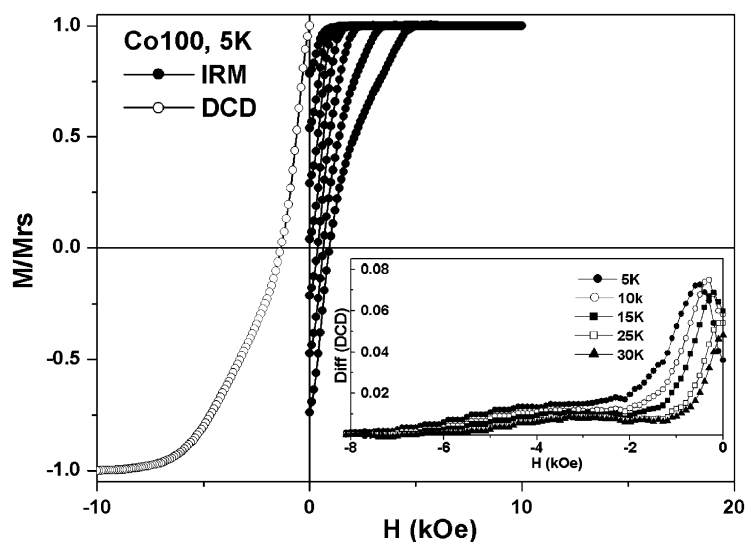


Fig. 2. The forward IRM and the DCD curve for the Co100 sample at $T = 5$ K. The inset shows the switching field distribution for the same sample at various temperatures.

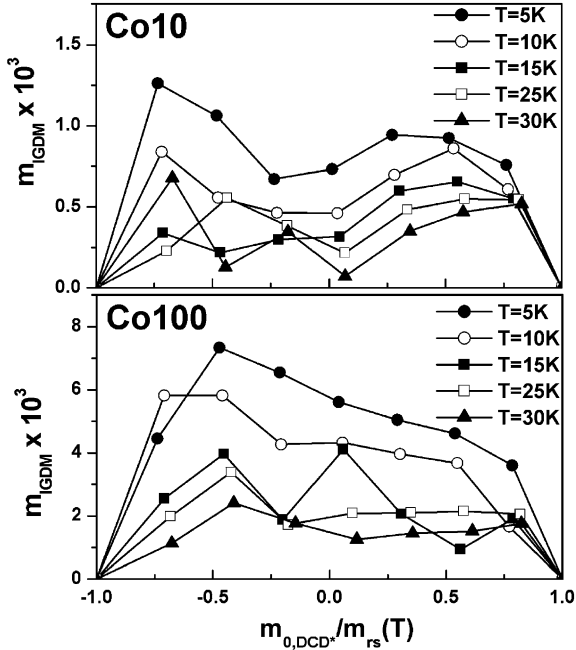


Fig. 3. The IGDMs for the Co100 (a) and Co10 (b) samples at various temperatures.

systems but to dynamical interactions [7]. The asymmetry of the IGDM curve could be explained by the asymmetric coercive field distribution. The switching field distributions (SFD), calculated as derivatives of the DCD curves, for different temperatures, confirm this asymmetry (see inset Fig. 2). Also, this is consistent with the extended tail of Co nanoparticle size distribution histogram determined by light scattering experiments. This can be explained by the existence in the studied samples not only of isolated Co nanoparticles but also of a small fraction of clusters of Co nanoparticles with a larger average diameter. The Co10 sample IGDMs are significantly different from the Co100 sample. They show a central minimum that separates two maxima. This is characteristic of systems in which the mean field or exchange interactions are more important than the static statistic interactions. It is easy to understand that the statistic interactions intensity in the Co10 sample is less important than in the Co100 sample, as the average distance between particle in the former sample is larger than in the latter one. The presence of exchange-type interactions in this

sample is probably linked with the presence of clusters in the system. As in the other case, the static interaction intensity, measured by the IGDM, is decreasing with the temperature increase.

3. Preisach-type model. Simulations

The generalized moving Preisach (GMP) model we used to simulate the temperature-dependent IGDMs is completely described by two distributions, (the irreversible Preisach distribution $P_i(H_\alpha, H_\beta)$, and a singular reversible Preisach distribution $P_r(H_\alpha)$ that is non-zero only on the first bisector of the Preisach plane) and the “moving” parameter [8]. We used instead of the switching fields (H_α, H_β) coordinate system the system denoted by (h_c, h_i) and rotated through 45° with respect to the first set where

$$h_c = (\sqrt{2}/2)(H_\alpha - H_\beta) \quad \text{and}$$

$$h_i = -(\sqrt{2}/2)(H_\alpha + H_\beta). \quad (2)$$

We assume that the coercive and interaction field distributions are statistically independent and that the coercive field distribution is log-normal with a Gaussian interaction field distribution. The irreversible part of the Preisach distribution is given by

$$p_i(h_c, h_i) = \frac{S}{2\pi h_{c\sigma} h_{i\sigma}} \left\{ \frac{1}{(h_c/h_{c0})} \exp \left[-\frac{\ln^2(h_c/h_{c0})}{2(h_{c\sigma}/h_{c0})^2} \right] \right\} \times \left\{ \exp \left[-\frac{h_i^2}{2h_{i\sigma}^2} \right] \right\} \quad (3)$$

and the reversible part

$$p_r(h_i) = \frac{(1-S)}{2h_{r\sigma}^2} \left\{ \exp \left[-\frac{|h_i|}{h_{r\sigma}} \right] \right\}, \quad (4)$$

where the following notations are used:

- S is the weight of the irreversible part;
- $h_{c\sigma}, h_{i\sigma}, h_{r\sigma}$ are parameters describing the dispersions of the coercivity, interaction and reversible part distributions, respectively;
- h_{c0} is related to the position of the maximum of the coercivity distribution (in fact, the position of the maximum, $h_{c,\max}$, is given by: $h_{c,\max} = h_{c0} \exp(-h_{c\sigma}^2/h_{c0}^2)$).

With this GMP model we have simulated the IGDM set of experimental data for the two samples, in a simplified manner. We wished to check if our assumption that the change in the statistical interactions due to blocked particles in the system can explain qualitatively the shape of the experimental data described in the previous section.

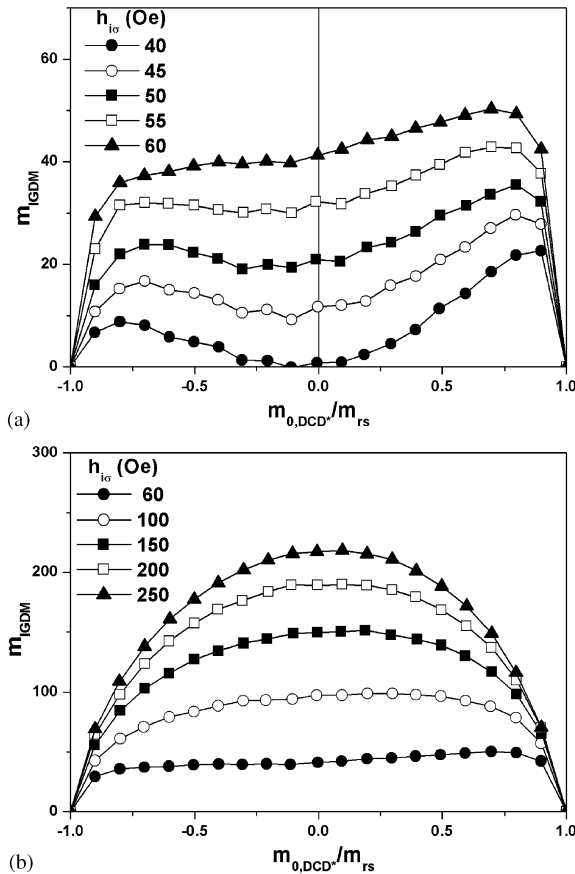


Fig. 4. (a) Simulated IGDM with the GMP model with log-normal distribution of the critical fields as in the formulae (3) and (4), with $S = 0.85$; $\alpha = 90$ Oe (the moving parameter); $h_{c0} = 1160$ Oe; $h_{c\sigma} = 300$ Oe; $h_{r\sigma} = 2262$ Oe; and for different values of the $h_{i\sigma}$ parameter describing the interactions distribution (40, 45, 50, 55 and 60 Oe). (b) Simulated IGDM with the GMP model with log-normal distribution of the critical fields as in the formulae (3) and (4), with $S = 0.85$; $\alpha = 90$ Oe (the moving parameter); $h_{c0} = 1160$ Oe; $h_{c\sigma} = 300$ Oe; $h_{r\sigma} = 2262$ Oe; and for different values of the $h_{i\sigma}$ parameter describing the interactions distribution (60, 100, 150, 200 and 250 Oe).

First we have simulated the IGDMs changing only the interaction field distribution dispersion. The two sets of simulated IGDMs presented in Figs. 4a and b show the same general shape as the experimental IGDMs from Fig. 3 (Fig. 4(a) for the Co10 sample and Fig. 4(b) for the Co100 sample). The main difference is that the simulated IGDMs have systematically greater values for positive values of the initial remanent moment than for the negative values while in the experimental IGDMs the curve has greater values for negative initial remanent states than for the positive ones. This is usually considered to be due to the asymmetry of the critical field distribution (log-normal in the simulations). As we can see from the SFD obtained by taking the derivative of the DCD curve, our system seems to have a peculiar critical field distribution with two maxima. We have changed the critical field distribution in the GMP model with the distribution:

$$P(h_c) = \frac{1}{2} \left[\frac{1}{\sqrt{2\pi}h_{c\sigma 1}} \exp\left(-\frac{(h_c - h_{c01})^2}{2h_{c\sigma 1}^2}\right) + \frac{1}{\sqrt{2\pi}h_{c\sigma 2}} \exp\left(-\frac{(h_c - h_{c02})^2}{2h_{c\sigma 2}^2}\right) \right]. \quad (5)$$

(Fig. 5 shows the graph of the distribution used in the second set of simulations.)

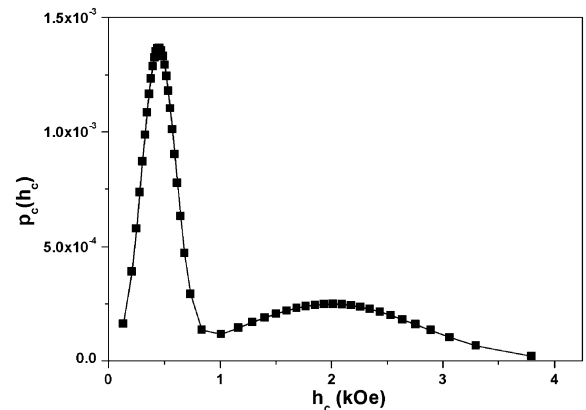


Fig. 5. Critical field distribution calculated with formula (5) with $S = 0.85$; $\alpha = 90$ Oe; $h_{c01} = 450$ Oe; $h_{c02} = 2000$ Oe; $h_{c\sigma 1} = 150$ Oe; $h_{c\sigma 2} = 800$ Oe.

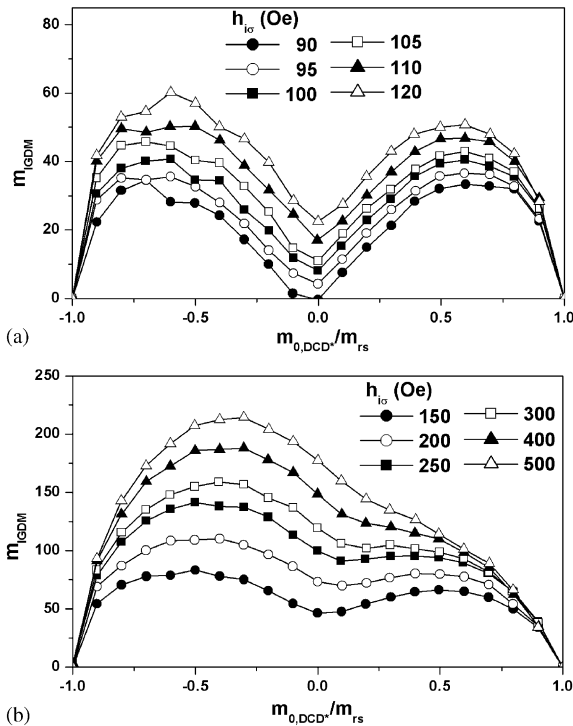


Fig. 6. (a) Simulated IGDM with the GMP model with log-normal distribution of the critical fields as in the formula (5), with $S = 0.85$; $\alpha = 90$ Oe; $h_{c01} = 450$ Oe; $h_{c02} = 2000$ Oe; $h_{c\sigma1} = 150$ Oe; $h_{c\sigma2} = 800$ Oe. $h_{rs} = 2262$ Oe; and for different values of the h_{is} parameter describing the interactions distribution (90, 95, 100, 105, 110 and 120 Oe). (b) Simulated IGDM with the GMP model with log-normal distribution of the critical fields as in the formula (5), with $S = 0.85$; $\alpha = 90$ Oe; $h_{c01} = 450$ Oe; $h_{c02} = 2000$ Oe; $h_{c\sigma1} = 150$ Oe; $h_{c\sigma2} = 800$ Oe. $h_{rs} = 2262$ Oe; and for different values of the h_{is} parameter describing the interactions distribution (150, 200, 250, 300, 400 and 500 Oe).

With the new critical field distribution extracted from the experimental SFD the IGDMs as a function of the static statistical field distribution dispersion the simulated set of IGDMs is a much better qualitative agreement with the experiment (see Figs. 6a and b).

4. Conclusions

In this paper, we have presented a new method of experimentally evaluating the interactions evolution as a function of temperature and system packing factor in nanoparticulate ensembles. IGDM simulated curves show the diminishing of the static interactions due to blocked particles as the temperature increasing and the packing factor decreasing. This was taken into account in Refs. [7,8] as a reasonable hypothesis for a Preisach–Néel model, but the results presented in this paper give a stronger motivation for that idea. The GMP model is able to describe this evolution of the IGDMs when the critical field distribution is taken as a function similar to the experimental SFD.

Acknowledgements

Work at AMRI was supported through NSF/LEQSF Grant No. (2001-04)-RII-03. Work in Iasi was supported by Romanian CNCSIS under the grants A/2000 and 2001 and D42

References

- [1] J.L. Dormann, D. Fiorani, E. Tronc, *Adv. Chem. Phys.* 98 (1997) 283.
- [2] A. Stancu, P.R. Bissell, R.W. Chantrell, *J. Magn. Magn. Mater.* 193 (1999) 395.
- [3] P.R. Bissell, M. Cerchez, R.W. Chantrell, Al. Stancu, *IEEE Trans. Magn.* 36 (2000) 2438.
- [4] A. Stancu, L. Stoleriu, M. Cerchez, *J. Magn. Magn. Mater.* 225 (2001) 411.
- [5] P.E. Kelly, K. O'Grady, P.I. Mayo, R.W. Chantrell, *IEEE Trans. Magn.* 25 (1989) 3881.
- [6] S. Sun, C.B. Murray, *J. Appl. Phys.* 85 (8) (1999) 4325.
- [7] Al. Stancu, L. Spinu, *IEEE Trans. Magn.* 34 (6) (1998) 3867.
- [8] Al. Stancu, P. Bissell, R. Chantrell, *J. Appl. Phys.* 87 (12) (2000) 8645.